Transcriptome profiling and functional analyses of the zebrafish embryonic innate immune response to Salmonella infection

Stockhammer, O.W.; Zakrzewska, A.; Hegedûs, Z.; Spaink, H.P.; Meijer, A.H.

The Journal of Immunology

RESEARCH ARTICLE | MAY 01 2009

Transcriptome Profiling and Functional Analyses of the Zebrafish Embryonic Innate Immune Response to *Salmonella* Infection [1]

Oliver W. Stockhammer; ... et. al

J Immunol (2009) 182 (9): 5641–5653.
https://doi.org/10.4049/jimmunol.0900082

Transcriptome Profiling and Functional Analyses of the Zebrafish Embryonic Innate Immune Response to *Salmonella* Infection[1]

Oliver W. Stockhammer,* Anna Zakrzewska,* Zoltán Hegedûs,† Herman P. Spaink,* and Annemarie H. Meijer[2]*

Due to the clear separation of innate immunity from adaptive responses, the externally developing zebrafish embryo represents a useful in vivo model for identification of innate host determinants of the response to bacterial infection. Here we performed a time-course transcriptome profiling study and gene ontology analysis of the embryonic innate immune response to infection with two model *Salmonella* strains that elicit either a lethal infection or an attenuated response. The transcriptional response to infection with both the lethal strain and the avirulent LPS O-Ag mutant strain showed clear conservation with host responses detected in other vertebrate models and human cells, including induction of genes encoding cell surface receptors, signaling intermediates, transcription factors, and inflammatory mediators. Furthermore, our study led to the identification of a large set of novel immune response genes and infection markers, the future functional characterization of which will support vertebrate genome annotation. From the time series and bacterial strain comparisons, matrix metalloproteinase genes, including *mmp9*, were among the most consistent infection-responsive genes. Purified *Salmonella* flagellin also strongly induced *mmp9* expression. Using knockdown analysis, we showed that this gene was downstream of the zebrafish homologs of the flagellin receptor TLR5 and the adaptor MyD88. Additionally, flagellin-mediated induction of other inflammation markers, including *il1b, il8*, and *cxcl-C1c*, was reduced upon Tlr5 knockdown as well as expression of *irak3*, a putative negative TLR pathway regulator. Finally, we showed that induction of *il1b*, *mmp9*, and *irak3* requires Myd88-dependent signaling, while *ifn1* and *il8* were induced Myd88 independently during *Salmonella* infection. *The Journal of Immunology,* 2009, 182: 5641–5653.

The innate immune system represents the evolutionary ancient part of vertebrate immunity and relies on germline-encoded receptors, commonly referred to as pattern recognition receptors, to mediate immune responses to pathogenic microorganisms. Triggering of these receptors activates a variety of signal transduction pathways ultimately resulting in large alterations of the host transcriptome profile, of which the dynamic complexity and underlying mechanisms are still poorly understood, especially at the whole organism level.

An essential class among the investigated pattern recognition receptors are the TLRs. Detection of microorganisms by TLRs is facilitated through specific interaction of the members of this family with evolutionary conserved microbial molecules that are not found in higher eukaryotes, for example, LPS from the outer membrane of Gram-negative bacteria (TLR4), flagellin from bacterial flagella (TLR5), or unmethylated CpG dinucleotides commonly found in bacterial DNA (TLR9) (1–3). Stimulation of TLRs by their ligands leads to the recruitment of adaptor proteins to the receptors. Differential utilization of the adaptor molecules by the TLRs causes specific activation of a range of transcription factors such as NF-κB, activator protein 1 (AP-1), and IFN regulatory factors (IRF) 3, 5, and 7 through distinct signaling pathways, eventually leading to the downstream activation of proinflammatory cytokines (4). To date, five adaptor proteins involved in TLR signaling have been described in humans: MyD88, MyD88 adaptor-like protein (Mal/TIRAP), Toll/IL-1 receptor (TIR) domain-containing adaptor protein inducing IFN-β (TRIF/TICAM1), TRIF-related adaptor molecule (TRAM/TICAM2), and sterile α- and armadillo motif-containing protein (SARM) (4). Among all adaptors, MyD88 is the most commonly used adaptor, and signaling through MyD88 has been implicated for all human TLRs with the exception of TLR3, which was shown to signal in a TRIF-dependent and MyD88-independent fashion (4, 5). Furthermore, MyD88 is involved in signal transduction of the IL-1 receptor and is associated with IFN-γ receptor signaling, leading to p38 activation (6, 7).

In recent years the zebrafish (*Danio rerio*) embryo system has emerged as a new model to study vertebrate innate immunity, offering several advantages that complement mammalian model systems. The transparent character of the externally fertilized zebrafish embryo in combination with fluorescently labeled immune cells and bacteria facilitate the study of host microbe interaction and inflammation processes in the living organism (8–14). The efficiency at which infections and chemical treatments in zebrafish can be performed at a large scale allows identification of novel microbial virulence factors and high throughput compound screens to investigate disease mechanisms (15, 16). Moreover, the zebrafish system is particularly

*Institute of Biology, Leiden University, Leiden, The Netherlands; and †ZenonBio, Szeged, Hungary, and Bioinformatics Laboratory, Biological Research Center, Hungarian Academy of Sciences, Szeged, Hungary

Received for publication January 12, 2009. Accepted for publication February 13, 2009.

The costs of publication of this article were defrayed in part by the payment of page charges. This article must therefore be hereby marked *advertisement* in accordance with 18 U.S.C. Section 1734 solely to indicate this fact.

[1] This work was supported by the European Commission Sixth Framework Programs ZF-MODELS (LSHG-CT-2003-503496) and ZF-TOOLS (LSHG-CT-2006-037220).

[2] Address correspondence and reprint requests to Dr. Annemarie H. Meijer, Institute of Biology, Leiden University, Einsteinweg 55, 2333 CC Leiden, The Netherlands. E-mail address: a.h.meijer@biology.leidenuniv.nl

suitable for large-scale forward and reverse genetic screens aimed at the identification of genes with novel functions in development of the immune system or in the immune response (17–19).

Analysis of the immune system of the zebrafish revealed a fully developed adaptive and innate immune system showing notable similarities to the mammalian equivalent (20–25). An active innate immune system is detectable already at day 1 of zebrafish embryogenesis demonstrated by the appearance of macrophages originating from the lateral plate mesoderm (26). Phagocytic activity of these cells was demonstrated upon bacterial encounter (8, 26, 27). In contrast, a functionally mature adaptive immune system is not active during the first 3 wk of zebrafish development (28–30). This clear temporal separation in zebrafish embryos provides a convenient system for in vivo study of the vertebrate innate immune response to infection independently from the adaptive immune response. To validate this model, we previously demonstrated that zebrafish embryos express a broad range of TLRs and adaptors. Furthermore, we demonstrated a conserved immune function for the TLR adaptor Myd88 by showing elevated susceptibility of the zebrafish embryo to an avirulent strain of *Salmonella enterica* serovar *Typhimurium* (hereafter referred to as *S. typhimurium*) upon morpholino-mediated knockdown (31). Zebrafish embryos also release conserved cytokines and chemokines, such as TNF-α, IL-1β, and IL-8, in response to bacterial infections (32, 33). Additionally, zebrafish embryos express a virus-induced IFN system ancestral to that of other vertebrates (34). However, knowledge of infection markers is still limited and the global transcriptional response to an infection has not been previously investigated in zebrafish embryos.

In recent years many infection systems for zebrafish have been developed (35–37). In this paper we used *S. typhimurium* as a case study for Gram-negative infections. An infection model for this well-studied human pathogen in zebrafish embryos has previously been established and it was demonstrated that an LPS mutant that shows an attenuated pathogenesis in mouse studies shows also attenuated infection in zebrafish embryos (9). Here we report on a time-resolved transcriptome profiling study of the zebrafish embryonic host immune response to *S. typhimurium* wild-type and LPS-mutant infection. Gene ontology comparisons of expression signatures in infections of zebrafish embryos and human and other vertebrate systems revealed a substantial overlap, further underscoring the validity of the zebrafish model. Furthermore, we identified a large set of novel immune response genes and infection markers, providing a strong basis for future research. Finally, we used infection markers resulting from this study to investigate the functions of Tlr5 and Myd88 by knockdown analysis using morpholino antisense oligonucleotides.

Materials and Methods

Bacterial strains and growth conditions

S. typhimurium wild-type (wt)[3] strain SL1027 and its isogenic LPS derivative SF1592 (*Ra*), both containing the DsRed expression vector pGMDs3, were used for the infection of zebrafish embryos (9). A nonflagellated derivative of this strain (*flhC*$^-$) contained an flhC::Mu*d*J insertion generously provided by K. Hughes (University of Utah) (38). Bacteria were freshly grown overnight on Luria-Bertani agar plates supplemented with 100 μg/ml carbenicillin (wt and Ra mutant strain) and 50 μg/ml kanamycin (*flhC*$^-$) and resuspended in PBS before injection.

Zebrafish husbandry

Zebrafish were handled in compliance with the local animal welfare regulations and maintained according to standard protocols (zfin.org). Embryos were grown at 28.5–30°C in egg water (60 μg/ml Instant Ocean sea salts). For the duration of bacterial injections embryos were kept under anesthesia in egg water containing 0.02% buffered 3-aminobenzoic acid ethyl ester (tricaine; Sigma-Aldrich). Embryos used for whole mount in situ staining were kept in egg water containing 0.003% 1-phenyl-2-thiourea (Sigma-Aldrich) to prevent melanization.

Morpholino knockdown experiments

For morpholino knockdown experiments, morpholino oligonucleotides (Gene Tools) were diluted to desired concentrations in 1× Danieu's buffer (58 mM NaCl, 0.7 mM KCl, 0.4 mM $MgSO_4$, 0.6 mM $Ca(NO_3)_2$, 5.0 mM HEPES (pH 7.6)) containing 1% phenol red (Sigma-Aldrich). To block translation of the *tlr5a*, *tlr5b*, or *myd88* mRNA, we injected 0.85 ng (0.1 mM), 4.2 ng (0.5 mM), and 8.4 ng (1 mM) per embryo, respectively. To control for aspecific morpholino effects, we used the standard control morpholino (0.6 mM) for the Tlr5 knockdown experiments and a previously described 5-bp mismatch morpholino (1 mM) (31) for the MyD88 knockdown studies. Morpholinos used target the 5′ untranslated region of the respective gene. Morpholino sequences are shown in supplemental Table I.[4]

Experimental design of infection study

All infection experiments were performed using mixed egg clutches from three tanks of AB strain zebrafish. Embryos were staged at 27 h postfertilization (hpf) by morphological criteria (39), and ~250 CFU of DsRed-expressing *S. typhimurium* wt and *Ra* mutant bacteria were injected into the caudal vein close to the urogenital opening. As a control an equal volume of PBS was likewise injected. Injections were controlled using a Leica MZ Fluo 3 stereomicroscope with epifluorescence attachment together with a FemtoJet microinjector (Eppendorf) and a micromanipulator with pulled microcapillary pipettes. Pools of 20–40 embryos were collected at 2, 5, 8, and 24 h postinfection (hpi). For the microarray analysis, the whole infection procedure was performed in triplicate on separate days. The order of injecting wt bacteria, *Ra* bacteria, and PBS control was randomized in the different experiments. Microarray analysis was performed using custom-designed 44K Agilent chips (Agilent Technologies). All *S. typhimurium* wt, *S. typhimurium Ra*, and PBS control RNA samples were labeled with Cy5 and hybridized against a Cy3-labeled common reference, which consisted of a mixture of all samples from the infection study.

Microarray design

The microarray slides were custom-designed by Agilent Technologies. The slides contained in total 43,371 probes of a 60-oligonucleotide length. Of these probes, a total of 21,496 probes were identical to the probes present on the Agilent probe set that is commercially available under catalog no. 013223_D. Most of the additional probes were designed using the eArray software from Agilent Technologies (earray.chem.agilent.com/earray). Settings used were based on the following settings: base composition methodology, best probe methodology, and design with 3′ bias. The Agilent *D. rerio* transcriptome was used as a reference database. A small number of probes were manually designed based on knowledge of particular polymorphisms for genes encoding protein families such as 14-3-3 proteins, chitinase-like proteins, and TLRs to obtain gene-specific probes. The microarray design has been submitted to the Gene Expression Omnibus database (www.ncbi.nlm.nih.gov/geo) under accession no. GPL7735.

RNA isolation, labeling, and hybridization

Embryos for RNA isolation were snap-frozen in liquid nitrogen and subsequently stored at −80°C. Embryos were homogenized in 1 ml of TRIzol reagent (Invitrogen), and subsequently total RNA was extracted according to the manufacturer's instructions. The RNA samples were incubated for 20 min at 37°C with 10 U of DNaseI (Roche Applied Science) to remove residual genomic DNA before purification using the RNeasy MinElute Cleanup kit (Qiagen) according to the RNA clean-up protocol. The integrity of the RNA was confirmed by lab-on-chip analysis using the 2100 Bioanalyzer (Agilent Technologies). Samples used for microarray analysis had an average RNA integrity number value of 9 and a minimum RNA integrity number value of 8.

Amino-allyl-modified amplified RNA (aRNA) was synthesized in one amplification round from 1 μg of total RNA using the Amino Allyl

[3] Abbreviations used in this paper: wt, wild type; BP, biological process; CC, cellular component; GO, gene ontology; hpf, hours postfertilization; hpi, hours postinfection; MF, molecular function; qRT-PCR, quantitative RT-PCR.

[4] The online version of this article contains supplemental material.

MessageAmp II aRNA Amplification kit (Ambion). Subsequently, 6 μg of amino-allyl-modified aRNA was used for coupling of monoreactive Cy3 and Cy5 dyes (GE Healthcare) and column purified. The dual-color hybridization of the microarray chips was performed at ServiceXS according to Agilent protocol G4140-90050 version 5.7 (www.Agilent.com) for two-color microarray-based gene expression analysis.

Data analysis

Microarray data were processed from raw data image files with Feature Extraction Software 9.5.3 (Agilent Technologies). Processed data were subsequently imported into Rosetta Resolver 7.0 (Rosetta Biosoftware) and subjected to default ratio error modeling. The raw data were submitted to the Gene Expression Omnibus database (www.ncbi.nlm.nih.gov/geo) under accession no. GSE13994. To compare *S. typhimurium* wt and *S. typhimurium Ra*-treated samples to the PBS-injected control samples a re-ratio experiment was performed using the Rosetta built-in re-ratio with common reference application. Data were analyzed at the level of UniGene clusters (UniGene build no. 105). Significance cut-offs for the ratios of wt vs PBS and Ra vs PBS were set at 1.5-fold change at $p < 10^{-4}$ for UniGene clusters. Two-dimensional hierarchical cluster analyses were performed with Rosetta Resolver settings for agglomerative algorithm (average link) with cosine correlation.

Gene ontology (GO) analysis was performed using the GeneTools *e*GOn v2.0 web-based gene ontology analysis software (www.genetools.microarray.ntnu.no) (40) and using Database for Annotation, Visualization and Integrated Discovery (DAVID) software tools (david.abcc.ncifcrf.gov/home.jsp) (41). GO analysis using *e*GOn was done at the level of the UniGene clusters (*D. rerio* UniGene build no. 105). GO analyses using DAVID tools were performed at the level of the Entrez Gene codes, because the DAVID database was not updated to a recent *D. rerio* UniGene build. To take advantage of the much better GO annotation of the human genome, we developed a software tool with which the UniGene and Entrez Gene records of the functionally related human homologs of our zebrafish UniGene list could be automatically retrieved from the National Center for Biotechnology Information (NCBI) HomoloGene database. Subsequently, *e*GOn and DAVID GO analyses were repeated using the UniGene (*Homo sapiens* UniGene build no. 202) and Entrez Gene lists of human orthologs, respectively. UniGene and Entrez Gene lists subjected to *e*GOn and DAVID analyses are included in supplemental Table II. Additionally, for comparison with human microarray data, the (putative) zebrafish homologs of the set of 511 human common host response genes described by Jenner and Young (42) were manually identified by searching the Zebrafish Information Network (ZFIN; zfin.org) and the Gene and HomoloGene databases of the NCBI (supplemental Table III). Homologs of human cytokines were identified based on phylogeny reconstructions to be reported elsewhere. Direct or putative homologs could be identified for 397 out of the 511 human common host response genes (78%), and 322 (63%) of these were represented on our zebrafish microarray. Since some genes are duplicated in zebrafish and since sometimes there was more than one putative homolog, there were 473 zebrafish UniGenes corresponding to the 322 human genes represented on the array.

Pathway analysis was performed using the Gene Map Annotator and Pathway Profiler (GenMAPP) software package (genmapp.org) (43). GenMAPP analysis was done at the level of UniGene clusters (*D. rerio* UniGene build no. 105). Significance cut-off was set at 1.5-fold change at $p < 10^{-4}$. Zebrafish homologs of the genes contributing to the TLR pathway were identified by either searching the ZFIN (zfin.org) database or the Gene and HomoloGene database of the NCBI (supplemental Table IV).

cDNA synthesis and quantitative real-time PCR

cDNA synthesis reactions were performed in a 20-μl mixture of 500 ng of RNA, 4 μl of 5× iScript reaction mix (Bio-Rad Laboratories), and 1 μl of iScript reverse transcriptase (Bio-Rad Laboratories). The reaction mixtures were incubated at 25°C for 5 min, 42°C for 30 min, and 85°C for 5 min.

Real-time PCR was performed using the Chromo4 Real-time PCR detection system (Bio-Rad Laboratories) according to the manufacturer's instructions. Each reaction was performed in a 25-μl volume comprised of 1 μl of cDNA, 12.5 μl of 2× iQ SYBR Green Supermix (Bio-Rad Laboratories), and 10 pmol of each primer. Cycling parameters were 95°C for 3 min to activate the polymerase, followed by 40 cycles of 95°C for 15 s and 59°C for 45 s. Fluorescence measurements were taken at the end of each cycle. Melting curve analysis was performed to verify that no primer dimers were amplified. All reactions were performed as technical duplicates. For normalization, peptidylprolyl isomerase A-like (*ppial*), which showed no changes over the infection time course series, was taken as reference (44). Results were analyzed using the $\Delta\Delta C_t$ method. Sequences of forward and reverse primers are described in supplemental Table I.

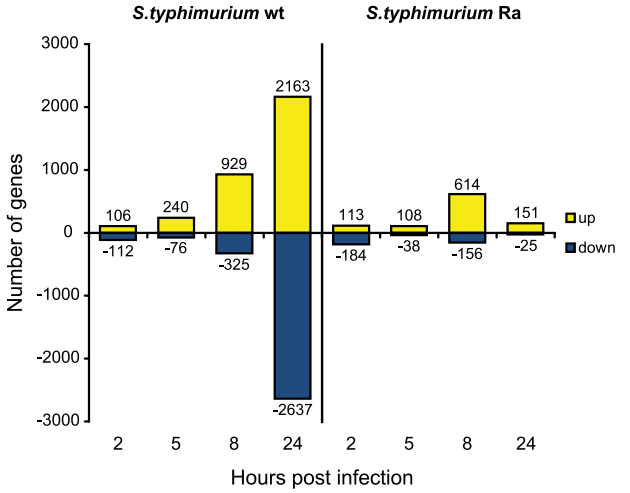

FIGURE 1. Temporal expression profiles of genes responsive to *S. typhimurium* wt and Ra infection. Total numbers of UniGene clusters that were significantly ($p \leq 10^{-4}$) up- or down-regulated (fold change $\geq$1.5 or ≤ -1.5) compared with the mock-injected control group at 2, 5, 8, and 24 hpi.

Whole-mount in situ hybridization

Embryos were fixed overnight in 4% paraformaldehyde in PBS at 4°C and whole-mount in situ hybridization using alkaline phosphatase detection with BM purple substrate (Roche) was performed according to Thisse et al. (45). Genomic DNA was used to generate templates for riboprobes synthesis by PCR using gene-specific primers sets including the binding site for T7 RNA polymerase in the reverse primer. Sequences of forward and reverse primers are described in supplemental Table I. Digoxigenin-labeled riboprobes were synthesized using the labeling mixes from Roche and Ambion MEGAscript reagents for in vitro transcription.

Results

Global changes in gene expression upon S. typhimurium *infection*

To characterize the host response of zebrafish embryos to bacterial infection, we performed a time-resolved transcriptome analysis of zebrafish embryos infected with either the *Salmonella typhimurium* wt strain LT2 or an isogenic LPS mutant (Ra) (9). Zebrafish embryos were systemically infected at the onset of blood circulation (27 hpf) by microinjection of 250 CFU of DsRed-labeled bacteria into the caudal vein or were mock injected with PBS. Injected embryos were sacrificed after incubation periods of 2, 5, 8, and 24 h, and microarray experiments were performed using a custom-designed 4 × 44K Agilent zebrafish platform. Datasets of three independent experiments revealed a strong response of the embryo to systemic infection with *S. typhimurium* compared with the mock-injected control group (Fig. 1 and supplemental Table II). The response to *S. typhimurium* wt was characterized by a gradually increasing number of responsive genes over the time course of the experiment, peaking at 24 hpi. A similar but attenuated response was visible for the Ra infection over the first 8 h. Furthermore, in contrast to the wt infection, a clear decline of responsive genes was observed at 24 hpi (Fig. 1). The temporal expression profiles correspond well to the course of *S. typhimurium* wt and Ra mutant infections in the zebrafish embryo as observed by fluorescence imaging. As shown in supplemental Fig. 1, the transient infection caused by the Ra mutant was nearly eliminated at 24 hpi, while a strong accumulation of DsRed-labeled wt bacteria was observed at 24 hpi, resulting in lethality around 30 hpi.

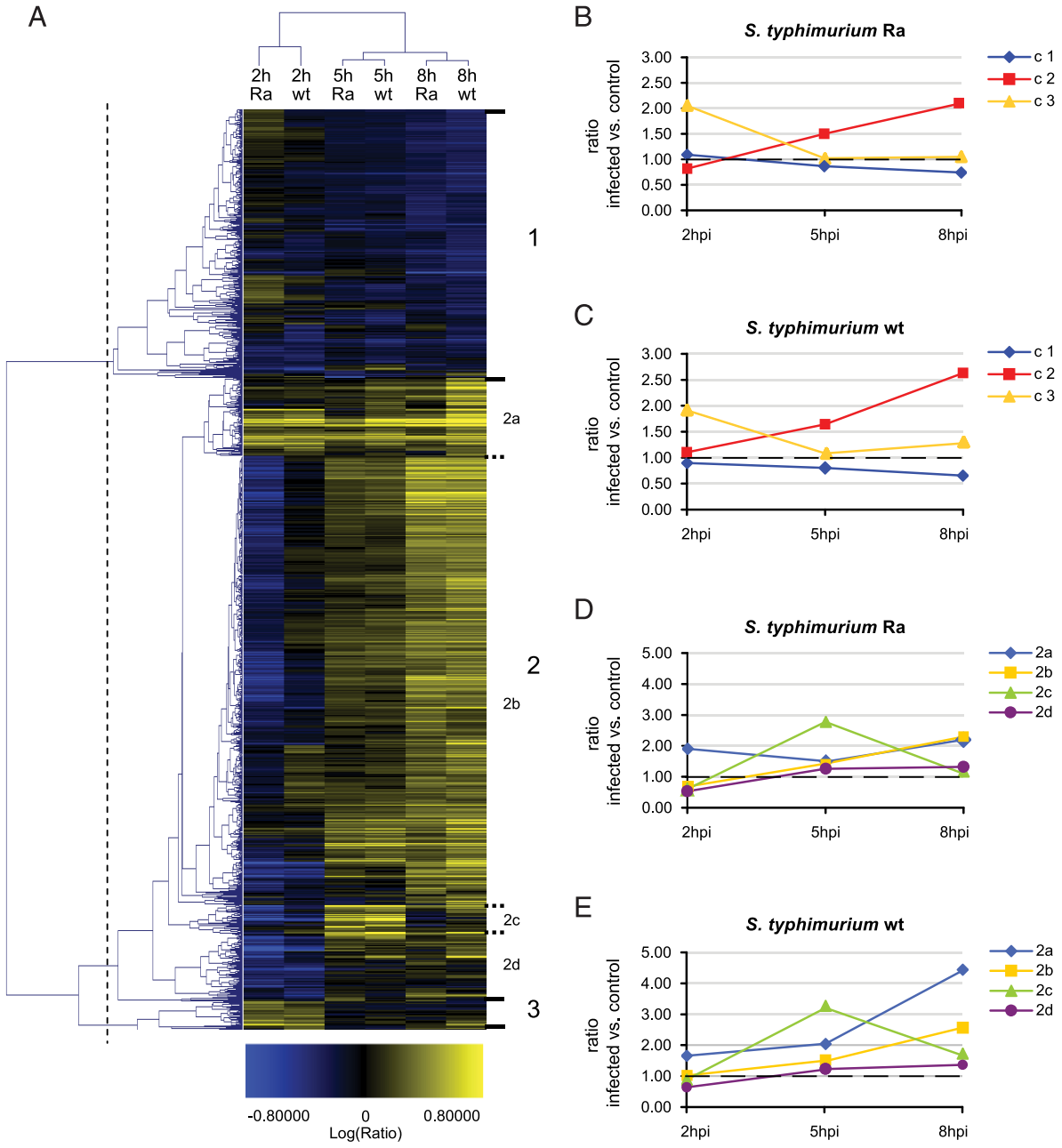

FIGURE 2. Trend analysis of gene expression patterns. *A*, Two-dimensional hierarchical clustering (average link, cosine correlation) performed on the UniGene clusters that were significantly up- or down-regulated during the first 8 h by wt and/or Ra infection. Induced genes are indicated by increasingly brighter shades of yellow, and down-regulated genes are indicated by increasingly brighter shades of blue. The three main clusters are named 1–3, and the four subclusters of cluster 2 are named 2a–2d. *B–E*, Trend graphs indicating the representative temporal expression profiles of the identified clusters. Average gene expression ratios at each time point upon *S. typhimurium* wt and Ra mutant infection are displayed for the three main clusters (*B* and *C*) and the four subclusters (*D* and *E*).

To further analyze the response to the wt and Ra strain over the first 8 h of the infection, we performed two-dimensional hierarchical cluster analysis. In the first dimension, the *S. typhimurium* wt and Ra infection profiles clustered together according to the experimental time points (Fig. 2*A*), indicating that zebrafish embryos respond similarly to infections with both strains. In the second dimension, we could distinguish three major clusters of genes showing different trends in expression over the time course (Fig. 2, *A–C* and supplemental Table V). Genes in cluster 1 exhibited a successive down-regulation over the first 8 h of the infection, whereas genes grouped in cluster 2 were generally induced over time. This cluster was further partitioned into four subclusters termed 2a–2d (Fig. 2, *A*, *D*, and *E*). Genes in cluster 2a showed induction over all time points. However, induction at 5 and 8 hpi was more pronounced after *S. typhimurium* wt infection. In contrast, genes in cluster 2b exhibited a broad down-regulation at 2 hpi followed by a successive up-regulation peaking at 8 hpi. In general, down-regulation of genes in cluster 2b was stronger for the Ra infection. A transient response was observed for genes in cluster 2c, showing an induction peak at 5 hpi followed by a decline at 8 hpi. Genes in cluster 2d showed a significant down-regulation at 2 hpi, followed by relatively low induction at 5 and 8 hpi. Finally, genes in cluster 3 showed a strong induction at 2 hpi with a subsequent decrease at 5 and 8 hpi.

A

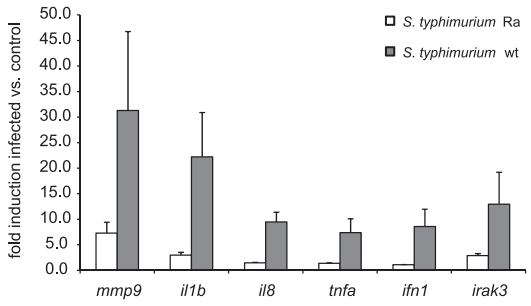

B

gene	treatment	qRT-PCR	microarray
mmp9	*S. typhimurium* wt *S. typhimurium* Ra	**+31.3** **+7.3**	**+22.5** **+6.5**
il1b	*S. typhimurium* wt *S. typhimurium* Ra	**+22.2** **+3.0**	**+10.1** **+2.6**
il8	*S. typhimurium* wt *S. typhimurium* Ra	**+9.5** **+1.5**	**+4.2** **+1.7**
tnfa	*S. typhimurium* wt *S. typhimurium* Ra	+7.4 +1.4	**+7.3** +1.9
ifn1	*S. typhimurium* wt *S. typhimurium* Ra	**+8.6** +1.1	**+7.6** +1.3
irak3	*S. typhimurium* wt *S. typhimurium* Ra	**+12.9** **+2.9**	**+4.0** **+2.5**

FIGURE 3. Validation of microarray data by qRT-PCR. Selected genes were analyzed on RNA samples from the 8 hpi time point previously used for the microarray experiment. qRT-PCR results were normalized to peptidylprolyl isomerase A-like (*ppial*), and data are presented as relative induction of the infected groups compared with the relevant mock-injected control groups. Values are the means ± SEM of three independent experiments. Fold changes determined by qRT-PCR and microarray experiment are listed in the table below the graph. Fold changes indicated in bold are significant with $p < 0.0001$ for the microarray data and $p < 0.05$ in an unpaired *t* test for the qRT-PCR data.

In conclusion, we observed a strong response to *S. typhimurium* infection in the zebrafish embryo with largely similar temporal expression profiles upon wt or Ra infection during the first 8 h after inoculation. Even though the Ra strain elicits only a transient infection and the wt infection becomes lethal, no gene groups with clearly anti-correlated behavior were revealed by hierarchical cluster analysis. Instead, differences in the host response to wt and Ra infection appeared to be limited to differences in trend at a single time point and to quantitative differences in up- or down-regulation.

Validation of microarray data by quantitative RT-PCR (qRT-PCR) and in situ hybridization

To validate the microarray data, qRT-PCR was performed on six genes that were significantly induced upon *S. typhimurium* infection (Fig. 3). The expression levels for *mmp9* (matrix metalloproteinase 9, NM_213123), *il1b* (IL-1β, NM_212844), *LOC100002946* (similar to IL-8, XM_001342570), hereafter referred to as *il8*, *tnfa* (TNF-α, NM_212859), *ifn1* (IFN-1, NM_207640), and *irak3* (IL-1 receptor-associated kinase 3, NM_001099421) were evaluated on the RNA samples of the 8 hpi time point previously used for the microarray study. The expression levels were normalized to *ppial* (NM_199957) (44), which showed no changes over the infection time course. Expression levels are presented as the relative induction in the infected group compared with the control group (Fig. 3*A*). In agreement with the microarray data, all genes tested in the qRT-PCR assay showed clear induction upon *S. typhimurium* wt infection and showed a lower response (*mmp9*, *il1b, il8*, and *irak3*) or no significant response (*tnfa*, *ifn1*) after infection with the Ra mutant (Fig. 3*B*).

In addition to the quantitative analysis by qRT-PCR, we also tested several genes by whole-mount in situ hybridization to further validate the microarray data and to add spatial information to the expression of infection-induced genes. Embryos were challenged with *S. typhimurium* wt by injection into the caudal vein close to the urogenital opening as in the microarray study. At 8 hpi the expression patterns of chemokine *cxcl-C1c* (LOC795785, AB331773.1), chemokine *ccl-C5a* (CH211-89F7.4, AB331770.1), *irak3*, and *socs3a* (suppressor of cytokine signaling 3a, NM_199950.1) were analyzed (Fig. 4, *A–D*). The selected genes were chosen on the criteria of a *p* value of $<10^{-5}$ and an induction >3-fold at 5 and 8 hpi. The *ccl-C5a* gene showed a specific expression pattern restricted to a narrow streak along the ventral side of the trunk, most likely representing the posterior region of the pronephric duct (Fig. 4*A*). Expression of *cxcl-C1c* (Fig. 4*B*) was predominantly visible in single cells located in the vascular system

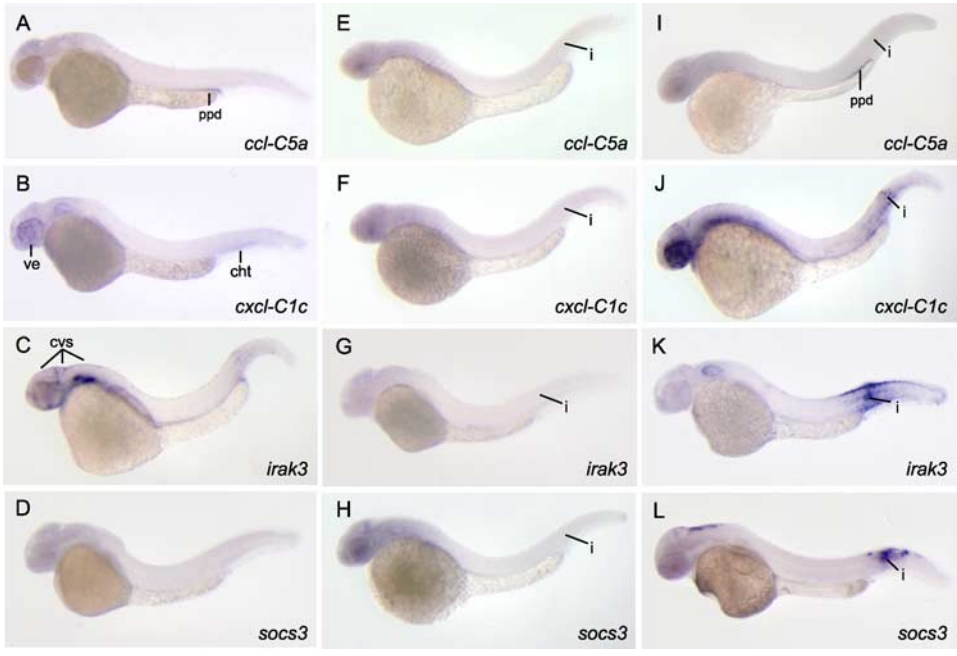

FIGURE 4. Analysis of spatial expression patterns of *S. typhimurium*-induced genes. Expression patterns of the indicated genes were analyzed at 8 hpi by whole-mount in situ hybridization. Embryos were injected at 27 hpf with *S. typhimurium* wt bacteria into the caudal vein (*A–D*), or injected with *S. typhimurium* wt bacteria into the somite tissue of the tail above the urogenital opening (*I–L*), or mock-injected with PBS at the same location (*E–H*). All embryos are oriented anterior to the left and dorsal to the top. cht, caudal hematopoietic tissue; cvs, cranial vascular system; i, location of injection into somite tissue; ppd, posterior pronephric duct; ve, vessels of the eye.

Table I. *Master-target test of GO analysis of up-regulated genes for biological process*[a]

GO Term	Name	Master	*S. typhimurium* Ra Mutant Target Lists				*S. typhimurium* wt Target Lists			
			2 h	5 h	8 h	24 h	2 h	5 h	8 h	24 h
Zebrafish UniGene identifiers										
GO:0008150	Biological process	6170	39	28	158	56	41	61	249	831
GO:0022610	Biological adhesion	74	0	0	0	0	1	0	1	9
GO:0065007	Biological regulation	1177	11	9	23	15	13	13	50	179
GO:0009987	Cellular process	3177	22	16	74	29	25	32	128	437
GO:0032502	Developmental process	653	4	4	8	5	5	4	21	94
GO:0051234	Establishment of localization	1138	3	3	29	6	5	7	47	160
GO:0040007	Growth	50	1	0	1	2	1	2	3	13
GO:0002376	Immune system process	72	**5**	**4**	4	**8**	**5**	**7**	**9**	**19**
GO:0051179	Localization	1195	3	3	29	6	6	7	47	167
GO:0040011	Locomotion	6	0	0	0	0	0	0	0	1
GO:0051235	Maintenance of localization	2	0	0	0	0	0	0	0	0
GO:0008152	Metabolic process	2493	19	12	63	24	18	25	100	351
GO:0051704	Multi-organism process	1	0	0	0	0	0	0	0	0
GO:0032501	Multicellular organismal process	633	3	7	9	6	4	6	18	68
GO:0043473	Pigmentation	13	0	0	0	0	0	0	0	0
GO:0000003	Reproduction	24	0	0	0	1	0	1	0	7
GO:0022414	Reproductive process	7	0	0	0	1	0	0	0	1
GO:0050896	Response to stimulus	213	5	**5**	8	**13**	5	**11**	**17**	**44**
GO:0048511	Rhythmic process	8	0	0	0	0	0	0	0	1
UniGene identifiers of human homologs										
GO:0008150	Biological process	5974	52	38	243	54	49	79	354	1319
GO:0022610	Biological adhesion	282	2	0	11	2	3	3	19	60
GO:0065007	Biological regulation	2079	22	13	**110**	25	**27**	30	**154**	**512**
GO:0001906	Cell killing	4	0	0	0	0	0	0	1	1
GO:0009987	Cellular process	5156	43	28	217	45	42	64	306	1140
GO:0032502	Developmental process	1402	16	8	41	15	**22**	18	81	322
GO:0051234	Establishment of localization	1132	7	10	45	14	7	19	73	259
GO:0040007	Growth	118	2	1	6	4	**5**	4	14	35
GO:0002376	Immune system process	230	**9**	**11**	**18**	**12**	**12**	**19**	**31**	**73**
GO:0051179	Localization	1290	8	10	51	14	8	20	80	287
GO:0040011	Locomotion	31	0	0	0	0	0	0	1	8
GO:0051235	Maintenance of localization	17	1	1	1	1	**2**	1	2	3
GO:0008152	Metabolic process	3899	29	22	177	34	31	48	244	877
GO:0051704	Multi-organism process	35	0	0	0	0	0	1	2	10
GO:0032501	Multicellular organismal process	1372	17	11	44	16	18	20	72	289
GO:0043473	Pigmentation	12	0	0	0	0	0	0	0	2
GO:0000003	Reproduction	178	3	1	3	0	0	3	9	39
GO:0022414	Reproductive process	88	1	1	2	0	0	2	4	20
GO:0050896	Response to stimulus	817	**15**	**12**	41	**18**	**17**	**23**	**67**	**225**
GO:0048511	Rhythmic process	34	0	0	1	0	0	1	1	8
GO:0016032	Viral reproduction	21	0	1	0	0	0	0	0	3

[a] A master-target statistical test using *e*GOn software was performed with input gene lists of zebrafish UniGene identifiers or the UniGene identifiers of their human homologs. The master input lists contained all UniGene identifiers present on the microarray (19,122 zebrafish UniGenes, for 10,620 of which the human homologs could be identified). The target lists contained the UniGene identifiers that were ≥1.5-fold up-regulated ($p \leq 0.0001$) at different time points of *S. typhimurium* wt or Ra mutant infection. The table indicates the number of genes in each list that are associated with the indicated GO terms. Numbers in boldface are significantly enriched in the target list compared to the master ($p < 0.01$). Note that genes can be associated with more than one GO term. For example, enrichment of the GO terms "development" and "growth" in the target list of *S. typhimurium* wt 2 h infection is due to the presence of genes such as *socs1* and *3*, *c7*, *il10*, *mmp9*, *fos*, *pim2*, and *nfkb2*, which also fall under the GO terms "immune response" and/or "esponse to stimulus".

of the embryonic eyes. A second area of elevated expression was observed around the caudal vein, also defined to single cells. Like *cxcl-C1c*, also the zebrafish homolog of *irak3* (Fig. 4*C*) showed an expression pattern restricted to the cranial vascular system of the embryo. However, a small number of embryos displayed a diverse pattern with a strong expression restricted to an area in the tail that corresponds with the site of the bacterial injection. To further investigate this observation we repeated the assay with a revised infection strategy. Bacteria were now locally injected into the somite tissue of the tail at 27 hpf leading to a confined accumulation of the bacteria at that site. Analysis of the expression pattern at 8 hpi confirmed the observed expression of *irak3* (Fig. 4*K*) in the tissue closely surrounding the infection site. Similarly, *socs3* also showed locally increased expression upon injection of bacteria into somite tissue (Fig. 4*L*). Local infection increased *ccl-C5a* (Fig. 4*I*) in the pronephric duct, similar to that observed upon blood infection (Fig. 4*A*); however, *ccl-C5a* expression did not accumulate around the infection site. In contrast, *cxcl-C1c* (Fig. 4*J*) did exhibit localized expression around the infection site, apparently restricted to single cells. To exclude the possibility that the observed expression patterns were provoked by local damage of the tissue that occurs upon bacterial injection, we also investigated the expression of all four genes in mock (PBS)-injected embryos (Fig. 4*E–H*). No signal was detected in the controls ($n = 5$ per gene) validating the specific host response toward the bacterial infection. Furthermore, the in situ hybridization results show that transcriptome profiling at the whole embryo level is highly suited to identify gene expression changes that are restricted to specific tissues or cell types.

Statistical testing for enrichment of gene ontology groups

To perform an unbiased functional annotation of the genes identified by microarray analysis we used *e*GOn, a web-based GO tool (40). The *e*GOn software classifies user input gene lists by GO criteria for biological process (BP), molecular function (MF), and

cellular component (CC); it produces hierarchical trees of GO terms in these three categories; and it allows statistical testing for enrichment or underrepresentation of specific GO terms in the input lists.

First we used the *e*GOn software to perform master-target statistical tests on the clusters of genes described above (Fig. 2), comparing the UniGene identifiers of each cluster (targets) vs all UniGene identifiers present on the chip (master). Master-target testing of the three main clusters (clusters 1–3 in Fig. 2) showed that the GO terms "immune system process" and "response to stimulus" at level 2 in the hierarchical tree for BP were significantly enriched in cluster 2, which contained the majority of the up-regulated genes. Next we analyzed the responses to the wt and Ra strains separately and at each individual time point of the infection. In agreement with the result obtained for cluster 2, master-target tests on the up-regulated UniGene sets showed that the BP GO terms "immune system process" and "response to stimulus" were significantly enriched at multiple time points of both the wt and Ra infections (Table I). In the MF tree, the level 2 GO term "enzyme regulator activity" was enriched (supplemental Table VI), and in the CC tree there was enrichment of GO terms associated with extracellular compartments (supplemental Table VII).

Although master-target testing of the up-regulated UniGenes identified several enriched GO terms with obvious relevance to an infection study, we noted that the number of UniGene identifiers associated with each of these GO terms was relatively low. We considered that this might be due to poor annotation of the zebrafish genome and that we might strengthen the results by performing a GO analysis of the human homologs of the zebrafish genes, thereby taking advantage of the much better annotated human genome. To this extent we developed a software tool with which the human homologs of the zebrafish UniGene list could be automatically retrieved from the NCBI HomoloGene database. Using this approach we could identify the human homologs of 56% of the zebrafish UniGene clusters present on the chip. As we had anticipated, the total number of associated GO terms was 1.6-fold higher. Furthermore, the relevant GO terms "immune system process" and "response to stimulus" were associated with 230 and 817 of all human homologs compared with only 72 and 213 of all zebrafish UniGenes. Repeating the master-target tests at the level of the human homologs showed that a larger number of genes were now associated with each of the enriched GO terms in the up-regulated signature sets of the infection time course. For example, in the *S. typhimurium* wt infection signature of 24 hpi there were 73 human homologs with the GO term "immune system process" compared with 19 zebrafish UniGenes, and 225 human homologs with the GO term "response to stimulus" compared with 44 zebrafish UniGenes (Table I). Additionally, the GO terms "biological regulation" (BP) and "transporter activity" (MF) were significantly enriched at multiple time points in the analysis of the human homologs, while not in the analysis of the zebrafish UniGenes.

For a more detailed GO analysis of the up- and down-regulated gene groups at the different time points of the infection study, we used the DAVID tools for functional classification and functional annotation clustering (41). The results of DAVID analyses are described in the supplemental material 1. In summary, DAVID analyses of the infections with both strains demonstrated rapid induction over the first 8 h of the time course of an increasing number of gene groups encoding transcription factors, signaling molecules, complement and acute-phase response proteins, proteinases and proteinase inhibitors, and solute carriers. At 24 hpi, the near-lethal wt infection led to the additional induction of apoptotic and antiapoptotic genes as well as negative regulators of cell cycle and proliferation, whereas gene groups involved in primary metabolic processes and DNA replication were down-regulated.

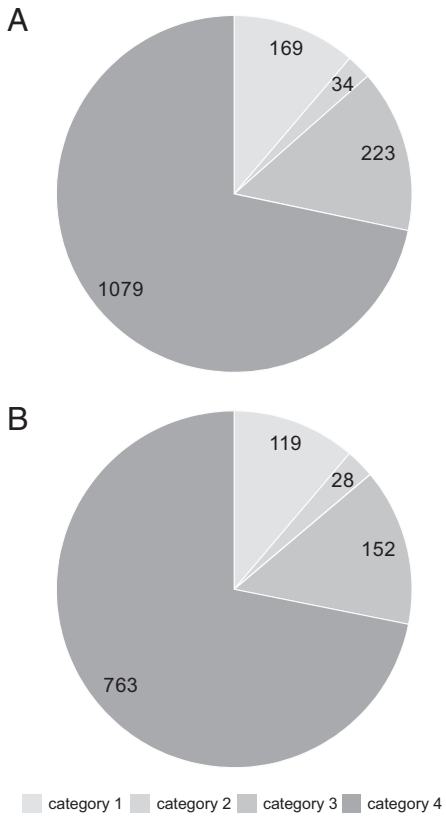

FIGURE 5. Identification of novel infection-responsive genes. All UniGene clusters regulated upon *S. typhimurium* wt (*A*) and Ra (*B*) challenge (infected vs control, $p \leq 0.0001$ and fold changes ≥ 1.5 and ≤ -1.5) were grouped into four categories: category 1, immune specific by means of GO annotation and overlap with the common host response genes in supplemental Table III; category 2, described immune function but missed out on category 1; category 3, functionally annotated but not associated to an immune function; category 4, no functional annotation. The numbers of UniGene clusters in each category are indicated in the pie diagrams.

Comparison with expression data from infection studies using human cell lines

To compare the *S. typhimurium*-induced gene profiles of zebrafish with gene profiles of infected human cell lines, we took advantage of a study by Jenner and Young (42), who systematically compared transcription profiling data from 32 studies that involved 77 different host-pathogen interactions. By cluster analysis of these data the authors identified an expression signature of 511 genes, which they designated "the common host response", as most of these genes were induced in many different human cell types upon exposure to several different pathogens. We sought to identify the zebrafish homologs of the genes in this common host response cluster using the ZFIN and NCBI Gene and HomoloGene databases, and found that 322 out of the 511 genes were represented on our zebrafish microarray. Of these, 39% were up-regulated (≥ 1.5-fold, $p < 0.0001$) at one or more time points of *S. typhimurium* wt and/or Ra infection (supplemental Table III). The overlap included genes encoding matrix metalloproteinases (e.g., *mmp9*, *mmp13*), adhesion molecules (e.g., *itga5*, *lgals9*), costimulatory molecules (e.g., CD83), Ag processing molecules (e.g., *tap2*, *psmb* family members), prostaglandin biosynthetic enzymes (e.g., *ptgs2*), signaling intermediates (e.g., *tradd*, *myd88*, *traf6*, *dusp* family members), apoptotic and antiapoptotic molecules (e.g., *casp* family

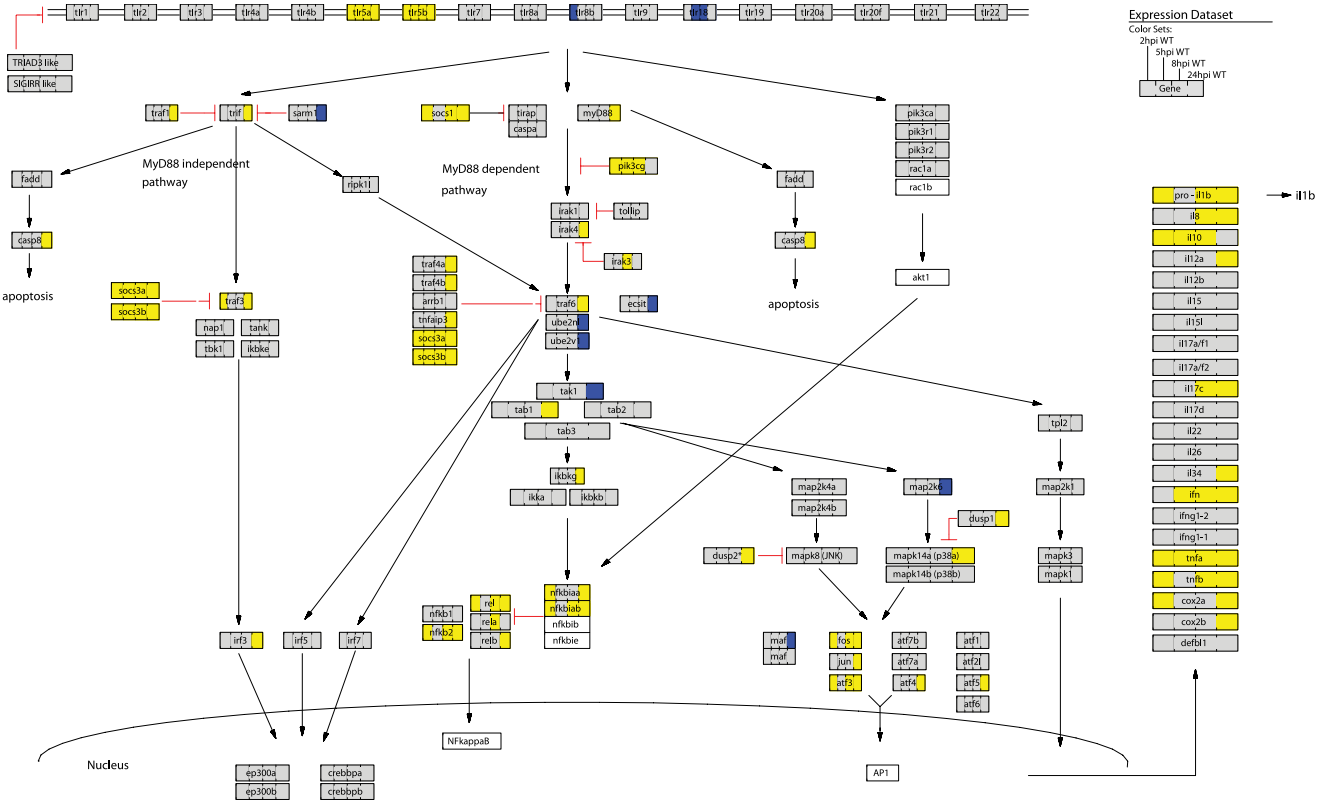

FIGURE 6. GenMAPP analysis of gene expression responses in the TLR pathway upon *S. typhimurium* wt infection. Expression profiles of the 2, 5, 8, and 24 hpi time points (infected vs control, $p \leq 0.0001$ and fold changes ≥ 1.5 and ≤ -1.5) were simultaneously mapped on the TLR pathway. Gene boxes are color coded from left to right with the 2, 5, 8, and 24 hpi expression data. Up-regulation is indicated in yellow, down-regulation in blue, and unchanged expression is indicated in gray. White denotes genes that were not represented on the array platform. The pathway is based on knowledge of TLR signaling in mammalian species. Note that most interactions remain to be experimentally confirmed in zebrafish. GenMAPP analysis of infection with the Ra mutant strain is shown in supplemental Fig. 2.

members, *mcl1*, *birc2*, *cflar*), transcription factors (e.g., members of the *NFκB*, *Jun*, *Fos*, *ATF*, *IRF*, and *STAT* families, *BCL6*, *Cebpg*, *xbp1*), IFNs and IFN-stimulated genes (e.g., *isg15* (*g1p2*), *mx1/2* homologs), and various chemotactic, proinflammatory, and other cytokines (e.g., homologs of *IL1β*, *IL8*, *IL10*, *TNF*, *TNFSF10*, *CCL* and *CXCL* chemokines). In conclusion, many important immune markers respond in a similar way in human cell cultures and in the early embryonic zebrafish system, thus allowing further functional in vivo studies of these genes.

Identification of novel putative immune response genes

As the next step we sought to determine which proportion of the genes regulated by *S. typhimurium* infection had not been previously linked to a function in the immune response. To this extent, we grouped all genes that were differentially expressed over the first 8 h of the infection time course (i.e., all genes included in the cluster analysis of Fig. 2) into four distinct categories (Fig. 5 and supplemental Table VIII). The first category contained all genes that were identified as immune specific by means of GO annotation and by overlap with the common host response gene set as described above (wt, 169 genes; Ra, 119 genes). In the second category we gathered those genes that have a described immune function in vertebrates but were missed in category 1, for example, *cebpb* and *socs3a* (wt, 34 genes; Ra, 28 genes). The third category consists of genes that were functionally annotated in zebrafish but were not yet linked to immune defense processes (wt, 223 genes; Ra, 152 genes). The remaining genes, grouped in category 4, still lack any functional annotation (wt, 1079 genes; Ra, 763 genes). The distribution of genes over the four categories (Fig. 5) shows that a substantial proportion (~50%) of all annotated genes that we identified upon *S. typhimurium* wt or Ra infection were correlated to an immune function (categories 1 and 2). Still, considering all genes that were regulated over the first 8 h upon infection, the majority of genes (~70%) have not yet been functionally characterized in the context of immunological processes and therefore represent novel putative immune response genes.

GenMAPP-based TLR pathway analysis reveals specific regulation of zebrafish Tlr5 and downstream signaling components

To further examine the immune response profiles of *S. typhimurium* wt and Ra infection at the level of a single signal transduction pathway, we performed a map-based pathway analysis using the GenMAPP software package (genmapp.org) (43). GenMAPP provides a platform to visualize gene expression datasets on customized maps of a desired signaling cascade and thereby allows the interpretation of gene expression changes in the context of a biological pathway. We used GenMAPP for the analysis of the TLR pathway, one of the most important pathways of the innate immune system (Fig. 6 and supplemental Fig. 2). Zebrafish homologs of the TLR pathway components used to create the GenMAPP were identified by searching the database of ZFIN (www.zfin.org) or the Gene and HomoloGene databases at the NCBI (www.ncbi.nlm.nih.gov) (supplemental Table IV). The responses upon *S. typhimurium* wt (Fig. 6) and Ra (supplemental Fig. 2) infection showed a similar trend between 2 and 8 hpi, with a strong initial response at 2 hpi (wt, 14 genes; Ra, 11 genes), a decrease at 5 hpi (wt, 6 genes; Ra, 2 genes) followed by a new

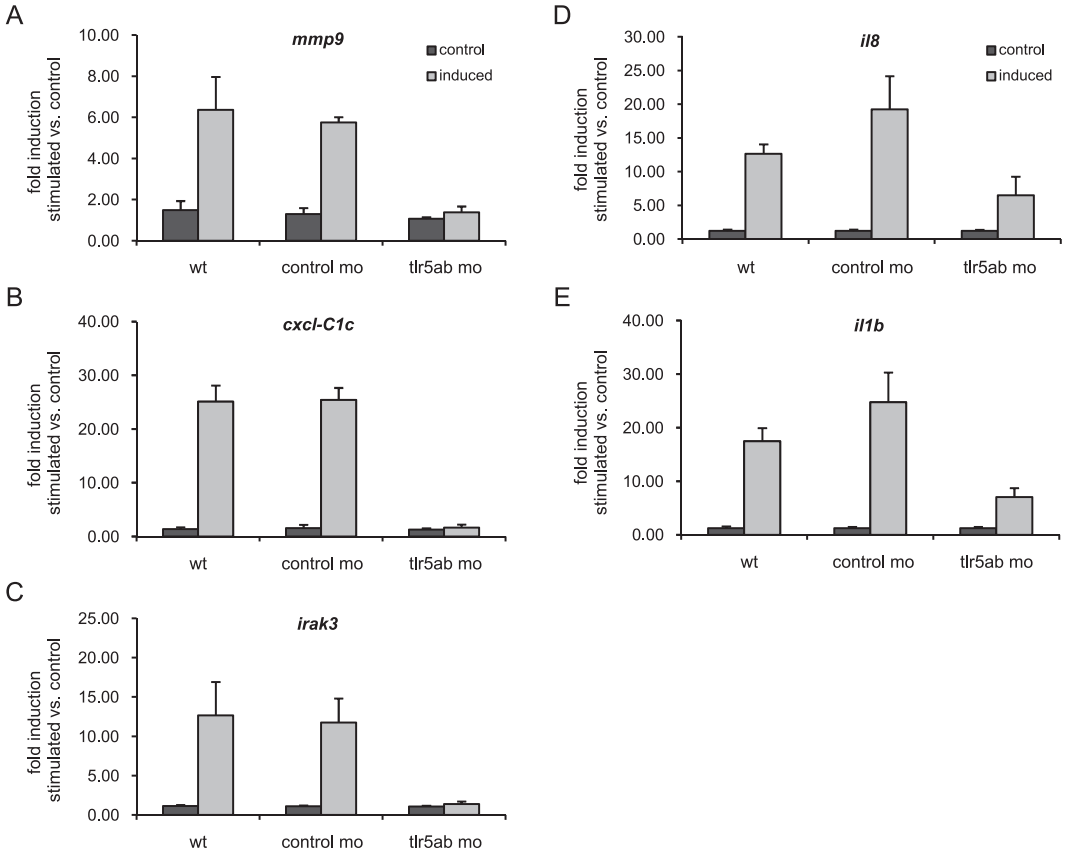

FIGURE 7. Response to *S. typhimurium* flagellin challenge in Tlr5a/b knockdown embryos. Embryos were injected at the single-cell stage with *tlr5a/b* or control morpholinos (mo) or were untreated (wt). The three groups were challenged at 27 hpf by flagellin injection or injection of toxin-free water as a control. Gene expression levels of *mmp9* (*A*), *cxcl-C1c* (*B*), *irak3* (*C*), *il8* (*D*), and *il1b* (*E*) at 1 hpi were determined by qRT-PCR and are shown as the fold induction of flagellin stimulation vs the water control. Values are the means ± SD of three independent experiments. The untreated and control mo groups did not behave significantly different. Differences between the *tlr5a/b* mo and control mo groups were significant by two-way ANOVA analysis ($p < 0.01$).

increase at 8 hpi (wt, 14 genes; Ra, 8 genes). At 24 hpi the wt infection peaked with 38 regulated genes, whereas the Ra infection showed a decline (4 genes), similar to what was observed for the global changes in gene expression described above (Fig. 1). GenMAPP analysis of the TLR pathway revealed a conserved pattern between wt and Ra-mediated infection. Both bacterial strains likewise induced the expression levels of genes encoding members of the NF-κB protein complex (*rel*, *rela*, *relb*, and *nfkb2*) that plays a key role in the transcriptional activation of proinflammatory cytokines (46). At the same time, also *nfkbiaa* and *nfkbiab* genes that encode the zebrafish homologs of the NF-κB transcription factor inhibitor NFKBIA are induced. Other transcription factor genes responsive to both strains include the *fos*, *jun, atf3*, *atf4*, and *atf5* genes encoding components of the AP-1 transcription factor complex. Genes that have been implicated in the negative regulation of the TLR pathway in higher vertebrates, such as *socs1*, s*ocs3a* and *socs3b*, *irak3*, *traf1*, and *pik3cg* (PI3Kγ), showed a clear activation from the earliest time point on. Finally, among the members of the TLRs that we previously identified in zebrafish (23), only *tlr5a* and *tlr5b* (the counterparts of the human *TLR5* gene) showed a broad up-regulation over the course of the infection.

Tlr5a/b is required for the activation of distinct host defense genes upon flagellin stimulation

Zebrafish *tlr5a* and *tlr5b* are two highly homologous genes located in tandem on chromosome 20 (Zv7_scaffold2018.4). To elucidate their role in the embryonic immune response, we performed knockdown experiments simultaneously using two morpholinos that specifically target the *tlr5a* and *tlr5b* mRNAs. Preliminary results indicated that Tlr5a/b was not required for the induction of inflammation markers such as *il1b*, *il8*, and *mmp9* upon *S. typhimurium* infection, which is not surprising since many other TLRs are involved in sensing of Gram-negative bacteria.

To further investigate Tlr5a/b function, we next addressed the question if the presumed ligand flagellin is able to elicit an immune response in the zebrafish embryo. Embryos were challenged by injection of 4 nl (100 μg/ml) of purified *S. typhimurium* flagellin (Invivogen) or solvent (toxin-free water) into the caudal vein at 27 hpf and the effect on expression of infection marker genes was investigated by qRT-PCR. Expression levels of *tlr5a*, *tlr5b*, *ifn1*, *irak3*, *il1b*, *il8*, *cxcl-C1c*, and *mmp9* were used as readout for qRT-PCR analyses. In wt embryos the expression of *il1b*, *il8*, *cxcl-C1c*, *mmp9*, and *irak3* was induced within 1 h of flagellin stimulation, while the expression of *tlr5a*, *tlr5b*, and *ifn1* was not induced over a time course of 5 h (Fig. 7 and supplemental Fig. 3). Results of three independent experiments showed that knockdown of Tlr5a/b led to an almost complete block of gene regulation of *mmp9*, *cxcl-C1c*, and *irak3* upon flagellin stimulation (Fig. 7, *A–C*). Furthermore, *il8* and *il1b* showed a reduced response to the flagellin challenge after *tlr5a/b* knockdown (Fig. 7, *D* and *E*). These data demonstrate that flagellin is a bona fide ligand of the zebrafish Tlr5a/b receptor and that Tlr5a/b plays a pivotal role in the activation of specific host defense genes upon stimulation.

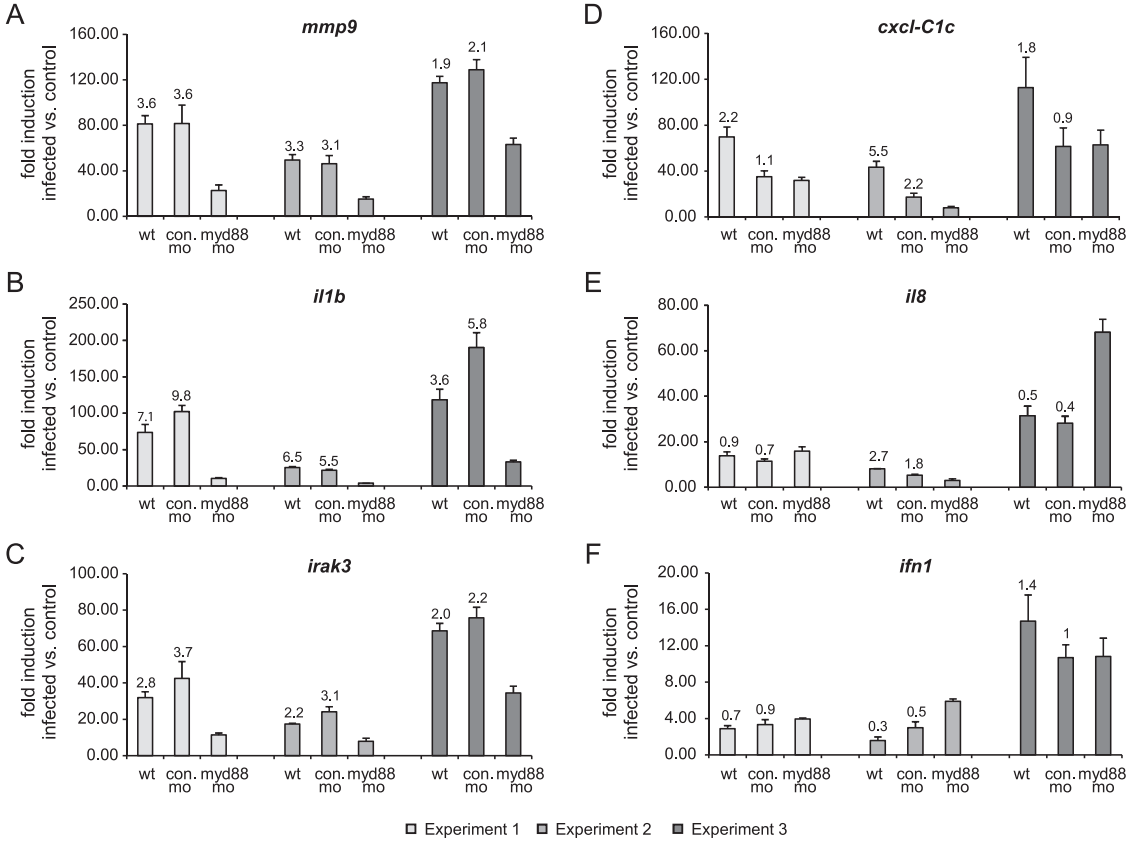

FIGURE 8. Response to *S. typhimurium* wt challenge in Myd88 knockdown embryos. Embryos were injected at the single-cell stage with *myd88* or control morpholinos (con. mo) or were untreated (wt). The three groups were infected at 27 hpf with *S. typhimurium* wt bacteria or mock-injected with PBS as a control. Gene expression levels of *mmp9* (*A*), *il1b* (*B*), *irak3* (*C*), *cxcl-C1c* (*D*), *il8* (*E*), and *ifn1* (*F*) at 8 hpi were determined by qRT-PCR and are shown as the fold induction of *S. typhimurium* infection vs the PBS control for all three experiments. The ratios of the untreated and the control group over the *myd88* morpholino group are indicated above the individual bars. The untreated and control morpholino groups did not behave significantly different with the exception of *cxcl-C1c*. Differences between the *myd88* morpholino and control morpholino groups were significant by an unpaired Student's *t* test ($p < 0.01$) for *mmp9*, *il1b*, and *irak3*.

MyD88 knockdown reveals MyD88-dependent and -independent gene activation upon bacterial infection

Signal transduction upon TLR stimulation is dependent on a group of five TIR domain-containing adaptor molecules. Among these, MyD88 is the most commonly used adaptor participating in signal transduction processes with all TLRs except TLR3 in mammals (4). To further investigate the role of the TLR pathway during bacterial infection, we performed *myd88* knockdown studies followed by *S. typhimurium* wt challenge and analyzed expression of the same infection marker set as used in the *tlr5* knockdown analysis. Due to the stochastic nature of bacterial infections, the absolute levels of gene induction that were observed upon *S. typhimurium* challenge varied considerably between different experiments. However, in three independent experiments, the induction levels of *mmp9*, *il1b*, and *irak3* expression were significantly reduced in the *myd88* morphants compared with nontreated embryos and embryos injected with the control morpholino (Fig. 8, *A–C*). Induction of *cxcl-C1c* was reduced in both mismatch control and *myd88* morphants, suggesting a currently unexplainable aspecific morpholino effect on the expression of this gene under infection conditions (Fig. 6*D*). Notably, no changes were observed for *ifn1* and *il8* expression, indicating a MyD88-independent activation of these genes (Fig. 6, *E* and *F*). Therefore, we conclude that the innate immune response of zebrafish embryos to *S. typhimurium* infection involves both MyD88-dependent and MyD88-independent signaling pathways.

Discussion

Herein we report the first time-resolved characterization of the immune response of a vertebrate embryo to a systemic bacterial infection at the transcriptome level. Aiming specifically at the analysis of innate host determinants, we took advantage of the clear temporal separation of the innate from the adaptive immune system in the externally developing zebrafish embryos (22, 28–30). In addition to the identification of a large set of genes that had not been previously linked to the immune response, we found a substantial overlap between the embryonic host response and immune responses measured in human and other vertebrate systems, indicating that the embryo model has a good predictive value for the vertebrate immunity. Furthermore, we present herein the first demonstration of a conserved TLR ligand specificity and the presence of MyD88-dependent and -independent signaling pathways in the zebrafish embryo.

The bacterial infection model used in this study is a previously described *S. typhimurium* system where a wt and an attenuated LPS O-Ag mutant strain (Ra) are utilized (9). Our transcriptome analysis of *S. typhimurium* wt and Ra mutant challenge demonstrated that both strains elicit a distinct temporal expression profile that is correlated to the symptoms of disease progression. Comparison of the host response during the first 8 h revealed similar expression trends for both strains despite the fact that the wt strain elicits a fatal infection, and the Ra mutant infection is cleared within a day. The main difference between the strains was

observed at 24 hpi, when the transcriptome response to the wt strain further increased and the response to the attenuated Ra mutant strain was on its return. The pathological differences are most likely due to a higher susceptibility of the Ra mutant to the embryonic immune response. As previously suggested, the complement system might be responsible for extracellular lysis of *S. typhimurium* LPS mutants observed in infected zebrafish embryos (9). In agreement, *S. typhimurium* O-Ag mutants showed higher susceptibility to complement lysis in in vitro studies (47, 48). The rapid induction of complement components like *c3b*, *c3c*, *c6*, and *cfb* (supplemental Table II) upon *S. typhimurium* challenge that we observed in our microarray study further supports the role of the complement system. Although there was a large overlap in the expression signatures of *S. typhimurium* wt and Ra infection during the first 8 h of the infection, most affected genes showed quantitative differences in expression levels, the functional implications of which are not yet understood. The transcriptome study reported herein provides a useful reference for future studies aimed at advancing the understanding of host-pathogen interactions.

Unbiased analysis of the infection datasets by two complementary annotation tools, *e*GOn and DAVID, clearly demonstrated an immune-specific host response of the zebrafish embryo to the *S. typhimurium* wt and Ra infections. Master-target testing performed by *e*GOn revealed the GO terms "immune system process" and "response to stimulus" as significantly enriched in the infection-up-regulated signature sets over the microarray background. However, fairly low numbers of genes were associated with these GO terms, which could be attributed to the still poor annotation of the zebrafish genome. We found that use of the NCBI HomoloGene database to convert the zebrafish UniGene identifiers to their predicted human homologs was a powerful tool to overcome this problem. Through their human homologs, >3-fold more zebrafish genes could be associated with the immune-specific GO terms. Additoinally, gene groups with a clear correlation to immune processes (i.e., "complement pathway" and "acute phase response") were identified by DAVID analysis by taking advantage of the human homolog conversion dataset. It remains to be experimentally confirmed if there is functional conservation between these unannotated zebrafish genes and their predicted human homologs; however, their up-regulation in response to *S. typhimurium* infection supports that they play a role in the host immune response.

The relevance of the zebrafish embryo model to study vertebrate immunity was further investigated by comparison of our transcriptome data to a meta-analysis of microarray data of various human cell lines challenged by different pathogens (42). We found a substantial overlap between the zebrafish host response to *S. typhimurium* and a set of genes that was commonly induced in all cell lines upon pathogen challenge referred to as "the common host response". The overlap included genes for well-known immune responsive transcription factors, cell surface receptors, signal transduction intermediates, adhesion factors, and proteins involved in tissue remodeling. Even though adaptive immunity is not yet developed in the zebrafish embryo, we also observed induction of genes encoding predicted zebrafish homologs of molecules involved in Ag processing and costimulation. Furthermore, various IFN, chemokine, proinflammatory cytokine, and antiinflammatory cytokine genes were shared between the gene sets of the zebrafish embryonic host response and the human common host response. Taken together, these observations further underscore the predictive value of the zebrafish embryo model.

TLRs are key players in the recognition of pathogens during host defense. We previously analyzed the zebrafish genome for genes encoding members of TLR signaling pathway leading to the identification of the zebrafish counterparts of the human TLRs and adapter proteins (23). GenMAPP-based analysis of the TLR pathway in this study demonstrated that various TLR signaling intermediates at different levels in the pathway are induced upon *S. typhimurium* wt and Ra infection in vivo. Genes implicated in the negative regulation of the pathway (e.g., *socs1*, *socs3*, and *pik3cg*) were among the earliest regulated genes (49–51). Additionally, we observed induction of genes encoding NF-κB inhibitors and the *irak3* gene, whose human homolog functions as a negative regulator of the TLR pathway (52). These observations suggest a tight regulation of the TLR pathway most likely to limit the potential negative consequences of excessive cytokine production. Furthermore, the zebrafish homologs of the human *TLR5*, *tlr5a* and *tlr5b*, were specifically up-regulated upon *S. typhimurium* wt and Ra challenge. It has previously been demonstrated that the mammalian TLR5 is mediating the immune response to bacterial flagellin (53), specifically recognizing conserved domains of monomeric flagellin crucial for bacterial motility and protofilament assembly (54). Our results showed that challenge of the zebrafish embryo with purified *S. typhimurium* flagellin elicited a strong activation of zebrafish homologs of the proinflammatory cytokine genes *IL-1β* and *IL-8*. Flagellin challenge also induced expression of the chemokine gene *cxcl-C1c,* the matrix metalloproteinase gene *mmp9*, and the putative negative regulator *irak3* discussed above. Functional assessment of *tlr5a* and *tlr5b* by morpholino-mediated knockdown followed by flagellin stimulation clearly demonstrated Tlr5-dependent gene activation of *mmp9*, *cxcl-C1c*, and *irak3* in the zebrafish embryo. Therefore, Tlr5 pathway activation appears to induce the expression of inflammatory mediators as well as feedback control of the innate immune response.

Although we found that flagellin induction of immune response genes was mediated by Tlr5, the *tlr5a* and *tlr5b* genes themselves were not induced upon flagellin stimulation. Furthermore, induction of *tlr5a* and *tlr5b* was still observed upon challenge with a nonflagellated derivative of the *S. typhimurium* wt strain (data not shown), demonstrating a flagellin-independent transcriptional activation of *tlr5a* and *tlr5b* during infection in the zebrafish embryo. Furthermore, preliminary results of knockdown experiments suggest that Tlr5 expression is not required for the induction of inflammatory mediators during *S. typhimurium* infection. This is consistent with observations in mice showing that TLR4 is able to compensate for the function of TLR5 upon *Salmonella* infection (55).

MyD88 functions as adaptor protein of TLR5 in mammalian systems and is also an important adaptor of other TLRs, including TLR4. In previous work we demonstrated the significance of Myd88 in the zebrafish embryo host defense by showing that accumulation of *S. typhimurium* Ra bacteria was increased upon Myd88 morpholino knockdown (31). Here, we extended this work and assessed transcriptional effects of Myd88 on downstream target genes of innate immunity signaling. Our results demonstrated a clear dependency of *mmp9*, *il1b*, and *irak3* on Myd88 for transcriptional activation upon *S. typhimurium* wt challenge. In contrast, *ifn1* and *il8* did not show changes in their induction upon bacterial challenge, demonstrating Myd88-independent activation of these genes. Differential use of the MyD88 adaptor in the TLR pathway is well documented in mammalian systems, with *IL1b* as the primary example of a MyD88-dependent target gene and *IFN* as a target of both MyD88-dependent and -independent routes (3, 4, 56). Our observations suggest a conserved mechanism in the zebrafish embryo. Furthermore, we have identified *mmp9* and *irak3* as novel MyD88-dependent immune response genes. MyD88-dependent as well as MyD88-independent induction of *IL-8* has been observed in mammalian systems (57, 58). However, regarding the Myd88-independent *il8* induction that we observed

in zebrafish embryos, note that the orthology of this gene with mammalian *IL-8* is ambiguous and that zebrafish express other closely related putative *IL-8* homologs.

In this study we found that that the matrix metalloproteinase genes *mmp9* and *mmp13* were among the strongest infection-responsive genes, with induction levels ~10- to 20-fold at 8 hpi for the *S. typhimurium* Ra and wt strains and >100-fold at 24 hpi for the *S. typhimurium* wt strain. Proteins of the mammalian matrix metalloproteinase family degrade extracellular matrices, thereby facilitating cell migration. Additionally, they are thought to affect the activity of inflammatory molecules (59). *S. typhimurium* and other bacterial species have been reported to secrete proteases that activate inactive proenzyme forms of matrix metalloproteinases, which may promote bacterial spreading through the host tissues (60). Here we have shown that *mmp9* expression is a target of the TLR5 pathway that is induced by *Salmonella* flagellin. Therefore, it appears that *Salmonella*-derived molecules can stimulate matrix metalloproteinase activity both at the transcriptional and the post-translational level. We have observed that induction of *mmp* genes is a common characteristic also of other types of bacterial infections in zebrafish, including *Edwardsiella*, *Pseudomonas*, and *Mycobacterium* infections (our unpublished results). Likewise, these genes are induced during pulmonary *Mycobacterium* infection in mice (61). Another metalloproteinase gene that we found induced upon *S. typhimurium* infection is *adam8* (a disintegrin and metalloproteinase domain 8), which belongs to a family of membrane-anchored glycoproteins that have been implicated in a variety of biological processes involving cell-cell and cell-matrix interactions. Recently, up-regulation of ADAM8 surface expression in human neutrophils was correlated with joint inflammation (62), and increased ADAM8 mRNA expression was also associated with allergic inflammation (63). The transparency of zebrafish embryos offers good possibilities to further investigate how gene expression of metalloproteinases such as the matrix metalloproteinases and ADAM8 contribute to tissue remodeling, inflammation, and bacterial dissemination.

Providing a case study for future immunity research in the zebrafish embryo model, our transcriptome analysis of the host response to *S. typhimurium* has linked a large set of zebrafish genes to the process of bacterial infection. Among these are a number of chemokine genes that have previously been annotated in the zebrafish genome, but that have not been functionally studied (64). Infection-responsive chemokine genes that were >3-fold induced over multiple time points of our in vivo infection study include *cxcl-C1c*, *cxcl-C5c*, *ccl-C5a*, *ccl-C24a*, and a chemokine gene weakly similar to *ccl-CUb* (Dr.125570). Another example of a putative immune response gene that we found to be strongly induced by *S. typhimurium* infection is the *zgc:65788* gene that encodes a homolog of the mammalian acidic chitinase family (5- to 10-fold at 8 hpi by the wt and Ra strains, and >30-fold at 24 hpi by the wt strain). Increased chitinase gene expression was also observed in our previous *Mycobacterium* infection study of adult zebrafish (65). There is increasing evidence for a role of acidic mammalian chitinases in Th2 inflammation and asthma (66, 67). The strong induction of *zgc:65788* expression during infection of zebrafish embryos suggests that chitinases may also play a role in the innate immune response. Finally, we found that ~70% of all genes that were specifically regulated during the first hours of *S. typhimurium* infection had not been previously linked to immunological processes. Many of these genes include transcribed loci that have unknown functions and for which the functions of their predicted human homologs are also unknown. With the possibility of performing rapid gene knockdown studies, the zebrafish embryo provides a useful model for the future functional characterization of these genes that will also support the further annotation of the human genome.

Acknowledgments

We are grateful to Astrid van der Sar (VU Medical Centre, the Netherlands) for providing DsRed-labeled *S. typhimurium* strains and for advice on infection experiments. We thank Wilbert Bitter (VU Medical Centre, the Netherlands), Ben Appelmelk (VU Medical Centre, the Netherlands), Kelly T. Hughes (University of Utah, USA), and Jelle Goeman (LUMC, the Netherlands) for helpful discussions as well as Marcel Schaaf, Ewa Snaar-Jagalska, and other members of the Institute of Biology. We are also grateful to Carianne Langerijs for testing in situ probes and to Davy de Witt and Ulrike Nehrdich for fish maintenance.

Disclosures

The authors have no financial conflicts of interest.

References

1. Medzhitov, R. 2001. Toll-like receptors and innate immunity. *Nat. Rev. Immunol.* 1: 135–145.
2. Beutler, B., and M. Rehli. 2002. Evolution of the TIR, tolls and TLRs: functional inferences from computational biology. *Curr. Top. Microbiol. Immunol.* 270: 1–21.
3. Kawai, T., and S. Akira. 2007. TLR signaling. *Semin. Immunol.* 19: 24–32.
4. O'Neill, L. A., and A. G. Bowie. 2007. The family of five: TIR-domain-containing adaptors in Toll-like receptor signalling. *Nat. Rev.* 7: 353–364.
5. Oshiumi, H., M. Matsumoto, K. Funami, T. Akazawa, and T. Seya. 2003. TICAM-1, an adaptor molecule that participates in Toll-like receptor 3-mediated interferon-β induction. *Nat. Immunol.* 4: 161–167.
6. Adachi, O., T. Kawai, K. Takeda, M. Matsumoto, H. Tsutsui, M. Sakagami, K. Nakanishi, and S. Akira. 1998. Targeted disruption of the MyD88 gene results in loss of IL-1- and IL-18-mediated function. *Immunity* 9: 143–150.
7. Sun, D., and A. Ding. 2006. MyD88-mediated stabilization of interferon-γ-induced cytokine and chemokine mRNA. *Nat. Immunol.* 7: 375–381.
8. Davis, J. M., H. Clay, J. L. Lewis, N. Ghori, P. Herbomel, and L. Ramakrishnan. 2002. Real-time visualization of mycobacterium-macrophage interactions leading to initiation of granuloma formation in zebrafish embryos. *Immunity* 17: 693–702.
9. Van der Sar, A. M., R. J. Musters, F. J. van Eeden, B. J. Appelmelk, C. M. Vandenbroucke-Grauls, and W. Bitter. 2003. Zebrafish embryos as a model host for the real time analysis of *Salmonella typhimurium* infections. *Cell. Microbiol.* 5: 601–611.
10. Ward, A. C., D. O. McPhee, M. M. Condron, S. Varma, S. H. Cody, S. M. Onnebo, B. H. Paw, L. I. Zon, and G. J. Lieschke. 2003. The zebrafish spi1 promoter drives myeloid-specific expression in stable transgenic fish. *Blood* 102: 3238–3240.
11. Redd, M. J., G. Kelly, G. Dunn, M. Way, and P. Martin. 2006. Imaging macrophage chemotaxis in vivo: studies of microtubule function in zebrafish wound inflammation. *Cell Motil. Cytoskeleton* 63: 415–422.
12. Renshaw, S. A., C. A. Loynes, D. M. Trushell, S. Elworthy, P. W. Ingham, and M. K. Whyte. 2006. A transgenic zebrafish model of neutrophilic inflammation. *Blood* 108: 3976–3978.
13. Mathias, J. R., B. J. Perrin, T. X. Liu, J. Kanki, A. T. Look, and A. Huttenlocher. 2006. Resolution of inflammation by retrograde chemotaxis of neutrophils in transgenic zebrafish. *J. Leukocyte Biol.* 80: 1281–1288.
14. Meijer, A. H., A. M. van der Sar, C. Cunha, G. E. Lamers, M. A. Laplante, H. Kikuta, W. Bitter, T. S. Becker, and H. P. Spaink. 2008. Identification and real-time imaging of a myc-expressing neutrophil population involved in inflammation and mycobacterial granuloma formation in zebrafish. *Dev. Comp. Immunol.* 32: 36–49.
15. Miller, J. D., and M. N. Neely. 2005. Large-scale screen highlights the importance of capsule for virulence in the zoonotic pathogen *Streptococcus iniae*. *Infect. Immun.* 73: 921–934.
16. Lieschke, G. J., and P. D. Currie. 2007. Animal models of human disease: zebrafish swim into view. *Nat. Rev. Genet.* 8: 353–367.
17. Schorpp, M., M. Bialecki, D. Diekhoff, B. Walderich, J. Odenthal, H. M. Maischein, A. G. Zapata, and T. Boehm. 2006. Conserved functions of Ikaros in vertebrate lymphocyte development: genetic evidence for distinct larval and adult phases of T cell development and two lineages of B cells in zebrafish. *J. Immunol.* 177: 2463–2476.
18. Trede, N. S., T. Ota, H. Kawasaki, B. H. Paw, T. Katz, B. Demarest, S. Hutchinson, Y. Zhou, C. Hersey, A. Zapata, et al. 2008. Zebrafish mutants with disrupted early T-cell and thymus development identified in early pressure screen. *Dev. Dyn.* 237: 2575–2584.
19. Pase, L., J. E. Layton, W. P. Kloosterman, D. Carradice, P. M. Waterhouse, and G. J. Lieschke. 2009. miR-451 regulates zebrafish erythroid maturation in vivo via its target gata2. *Blood* 113: 1794–1804.
20. Yoder, J. A., M. E. Nielsen, C. T. Amemiya, and G. W. Litman. 2002. Zebrafish as an immunological model system. *Microbes Infect.* 4: 1469–1478.
21. Traver, D., P. Herbomel, E. E. Patton, R. D. Murphey, J. A. Yoder, G. W. Litman, A. Catic, C. T. Amemiya, L. I. Zon, and N. S. Trede. 2003. The zebrafish as a model organism to study development of the immune system. *Adv. Immunol.* 81: 253–330.

22. Trede, N. S., D. M. Langenau, D. Traver, A. T. Look, and L. I. Zon. 2004. The use of zebrafish to understand immunity. *Immunity* 20: 367–379.
23. Meijer, A. H., S. F. G. Krens, I. A. Medina Rodriguez, S. He, W. Bitter, B. E. Snaar-Jagalska, and H. P. Spaink. 2004. Expression analysis of the Toll-like receptor and TIR domain adaptor families of zebrafish. *Mol. Immunol.* 40: 773–783.
24. Stein, C., M. Caccamo, G. Laird, and M. Leptin. 2007. Conservation and divergence of gene families encoding components of innate immune response systems in zebrafish. *Genome Biol.* 8: R251.
25. Murayama, E., K. Kissa, A. Zapata, E. Mordelet, V. Briolat, H. F. Lin, R. I. Handin, and P. Herbomel. 2006. Tracing hematopoietic precursor migration to successive hematopoietic organs during zebrafish development. *Immunity* 25: 963–975.
26. Herbomel, P., B. Thisse, and C. Thisse. 1999. Ontogeny and behaviour of early macrophages in the zebrafish embryo. *Development* 126: 3735–3745.
27. Herbomel, P., B. Thisse, and C. Thisse. 2001. Zebrafish early macrophages colonize cephalic mesenchyme and developing brain, retina, and epidermis through a M-CSF receptor-dependent invasive process. *Dev. Biol.* 238: 274–288.
28. Willett, C. E., A. Cortes, A. Zuasti, and A. G. Zapata. 1999. Early hematopoiesis and developing lymphoid organs in the zebrafish. *Dev. Dyn.* 214: 323–336.
29. Davidson, A. J., and L. I. Zon. 2004. The "definitive" (and "primitive") guide to zebrafish hematopoiesis. *Oncogene* 23: 7233–7246.
30. Lam, S. H., H. L. Chua, Z. Gong, T. J. Lam, and Y. M. Sin. 2004. Development and maturation of the immune system in zebrafish, *Danio rerio*: a gene expression profiling, in situ hybridization and immunological study. *Dev. Comp. Immunol.* 28: 9–28.
31. Van der Sar, A. M., O. W. Stockhammer, L. C. van der, H. P. Spaink, W. Bitter, and A. H. Meijer. 2006. MyD88 innate immune function in a zebrafish embryo infection model. *Infect. Immun.* 74: 2436–2441.
32. Pressley, M. E., P. E. Phelan, III, P. E. Witten, M. T. Mellon, and C. H. Kim. 2005. Pathogenesis and inflammatory response to *Edwardsiella tarda* infection in the zebrafish. *Dev. Comp. Immunol.* 29: 501–513.
33. Clay, H., H. E. Volkman, and L. Ramakrishnan. 2008. Tumor necrosis factor signaling mediates resistance to mycobacteria by inhibiting bacterial growth and macrophage death. *Immunity* 29: 283–294.
34. Levraud, J. P., P. Boudinot, I. Colin, A. Benmansour, N. Peyrieras, P. Herbomel, and G. Lutfalla. 2007. Identification of the zebrafish IFN receptor: implications for the origin of the vertebrate IFN system. *J. Immunol.* 178: 4385–4394.
35. Phelps, H. A., and M. N. Neely. 2005. Evolution of the zebrafish model: from development to immunity and infectious disease. *Zebrafish* 2: 87–103.
36. Meeker, N. D., and N. S. Trede. 2008. Immunology and zebrafish: spawning new models of human disease. *Dev. Comp. Immunol.* 32: 745–757.
37. Lesley, R., and L. Ramakrishnan. 2008. Insights into early mycobacterial pathogenesis from the zebrafish. *Curr. Opin. Microbiol.* 11: 277–283.
38. Chilcott, G. S., and K. T. Hughes. 2000. Coupling of flagellar gene expression to flagellar assembly in *Salmonella enterica* serovar *typhimurium* and *Escherichia coli*. *Microbiol. Mol. Biol. Rev.* 64: 694–708.
39. Kimmel, C. B., W. W. Ballard, S. R. Kimmel, B. Ullmann, and T. F. Schilling. 1995. Stages of embryonic development of the zebrafish. *Dev. Dyn.* 203: 253–310.
40. Beisvag, V., F. K. Junge, H. Bergum, L. Jolsum, S. Lydersen, C. C. Gunther, H. Ramampiaro, M. Langaas, A. K. Sandvik, and A. Laegreid. 2006. GeneTools: application for functional annotation and statistical hypothesis testing. *BMC Bioinformatics* 7: 470.
41. Dennis, G., Jr., B. T. Sherman, D. A. Hosack, J. Yang, W. Gao, H. C. Lane, and R. A. 2003. Lempicki. DAVID: Database for Annotation, Visualization, and Integrated Discovery. *Genome Biol.* 4: P3.
42. Jenner, R. G., and R. A. Young. 2005. Insights into host responses against pathogens from transcriptional profiling. *Nat. Rev. Microbiol.* 3: 281–294.
43. Dahlquist, K. D., N. Salomonis, K. Vranizan, S. C. Lawlor, and B. R. Conklin. 2002. GenMAPP, a new tool for viewing and analyzing microarray data on biological pathways. *Nat. Genet.* 31: 19–20.
44. Roesner, A., T. Hankeln, and T. Burmester. 2006. Hypoxia induces a complex response of globin expression in zebrafish (*Danio rerio*). *J. Exp. Biol.* 209: 2129–2137.
45. Thisse, C., B. Thisse, T. F. Schilling, and J. H. Postlethwait. 1993. Structure of the zebrafish snail1 gene and its expression in wild-type, spadetail and no tail mutant embryos. *Development* 119: 1203–1215.
46. Medzhitov, R., P. Preston-Hurlburt, and C. A. Janeway, Jr. 1997. A human homologue of the *Drosophila* Toll protein signals activation of adaptive immunity. *Nature* 388: 394–397.
47. Ohno, A., Y. Isii, K. Tateda, T. Matumoto, S. Miyazaki, S. Yokota, and K. Yamaguchi. 1995. Role of LPS length in clearance rate of bacteria from the bloodstream in mice. *Microbiology* 141(Pt 10): 2749–2756.
48. Murray, G. L., S. R. Attridge, and R. Morona. 2003. Regulation of *Salmonella typhimurium* lipopolysaccharide O antigen chain length is required for virulence; identification of FepE as a second Wzz. *Mol. Microbiol.* 47: 1395–1406.
49. Mansell, A., R. Smith, S. L. Doyle, P. Gray, J. E. Fenner, P. J. Crack, S. E. Nicholson, D. J. Hilton, L. A. O'Neill, and P. J. Hertzog. 2006. Suppressor of cytokine signaling 1 negatively regulates Toll-like receptor signaling by mediating Mal degradation. *Nat. Immunol.* 7: 148–155.
50. Frobose, H., S. G. Ronn, P. E. Heding, H. Mendoza, P. Cohen, T. Mandrup-Poulsen, and N. Billestrup. 2006. Suppressor of cytokine signaling-3 inhibits interleukin-1 signaling by targeting the TRAF-6/TAK1 complex. *Mol. Endocrinol.* 20: 1587–1596.
51. Liew, F. Y., D. Xu, E. K. Brint, and L. A. O'Neill. 2005. Negative regulation of Toll-like receptor-mediated immune responses. *Nat. Rev.* 5: 446–458.
52. Kobayashi, K., L. D. Hernandez, J. E. Galan, C. A. Janeway, Jr., R. Medzhitov, and R. A. Flavell. 2002. IRAK-M is a negative regulator of Toll-like receptor signaling. *Cell* 110: 191–202.
53. Hayashi, F., K. D. Smith, A. Ozinsky, T. R. Hawn, E. C. Yi, D. R. Goodlett, J. K. Eng, S. Akira, D. M. Underhill, and A. Aderem. 2001. The innate immune response to bacterial flagellin is mediated by Toll-like receptor 5. *Nature* 410: 1099–1103.
54. Smith, K. D., E. Andersen-Nissen, F. Hayashi, K. Strobe, M. A. Bergman, S. L. Barrett, B. T. Cookson, and A. Aderem. 2003. Toll-like receptor 5 recognizes a conserved site on flagellin required for protofilament formation and bacterial motility. *Nat. Immunol.* 4: 1247–1253.
55. Feuillet, V., S. Medjane, I. Mondor, O. Demaria, P. P. Pagni, J. E. Galan, R. A. Flavell, and L. Alexopoulou. 2006. Involvement of Toll-like receptor 5 in the recognition of flagellated bacteria. *Proc. Natl. Acad. Sci. USA* 103: 12487–12492.
56. Seki, E., H. Tsutsui, H. Nakano, N. Tsuji, K. Hoshino, O. Adachi, K. Adachi, S. Futatsugi, K. Kuida, O. Takeuchi, et al. 2001. Lipopolysaccharide-induced IL-18 secretion from murine Kupffer cells independently of myeloid differentiation factor 88 that is critically involved in induction of production of IL-12 and IL-1β. *J. Immunol.* 166: 2651–2657.
57. Balloy, V., J. M. Sallenave, Y. Wu, L. Touqui, J. P. Latge, M. Si-Tahar, and M. Chignard. 2008. *Aspergillus fumigatus*-induced interleukin-8 synthesis by respiratory epithelial cells is controlled by the phosphatidylinositol 3-kinase, p38 MAPK, and ERK1/2 pathways and not by the Toll-like receptor-MyD88 pathway. *J. Biol. Chem.* 283: 30513–30521.
58. Zheng, J., J. Meng, S. Zhao, R. Singh, and W. Song. 2008. *Campylobacter*-induced interleukin-8 secretion in polarized human intestinal epithelial cells requires *Campylobacter*-secreted cytolethal distending toxin- and Toll-like receptor-mediated activation of NF-κB. *Infect. Immun.* 76: 4498–4508.
59. Parks, W. C., C. L. Wilson, and Y. S. Lopez-Boado. 2004. Matrix metalloproteinases as modulators of inflammation and innate immunity. *Nat. Rev. Immunol.* 4: 617–629.
60. Ramu, P., L. A. Lobo, M. Kukkonen, E. Bjur, M. Suomalainen, H. Raukola, M. Miettinen, I. Julkunen, O. Holst, M. Rhen, et al. 2008. Activation of pro-matrix metalloproteinase-9 and degradation of gelatin by the surface protease PgtE of *Salmonella enterica* serovar *Typhimurium*. *Int. J. Med. Microbiol.* 298: 263–278.
61. Taylor, J. L., J. M. Hattle, S. A. Dreitz, J. M. Troudt, L. S. Izzo, R. J. Basaraba, I. M. Orme, L. M. Matrisian, and A. A. Izzo. 2006. Role for matrix metalloproteinase 9 in granuloma formation during pulmonary *Mycobacterium tuberculosis* infection. *Infect. Immun.* 74: 6135–6144.
62. Gomez-Gaviro, M., M. Dominguez-Luis, J. Canchado, J. Calafat, H. Janssen, E. Lara-Pezzi, A. Fourie, A. Tugores, A. Valenzuela-Fernandez, F. Mollinedo, et al. 2007. Expression and regulation of the metalloproteinase ADAM-8 during human neutrophil pathophysiological activation and its catalytic activity on L-selectin shedding. *J. Immunol.* 178: 8053–8063.
63. Matsuno, O., T. Kumamoto, and Y. Higuchi. 2008. ADAM8 in allergy. *Inflamm. Allergy Drug Targets* 7: 108–112.
64. Nomiyama, H., K. Hieshima, N. Osada, Y. Kato-Unoki, K. Otsuka-Ono, S. Takegawa, T. Izawa, A. Yoshizawa, Y. Kikuchi, S. Tanase, et al. 2008. Extensive expansion and diversification of the chemokine gene family in zebrafish: identification of a novel chemokine subfamily CX. *BMC Genomics* 9: 222.
65. Meijer, A. H., F. J. Verbeek, E. Salas-Vidal, M. Corredor-Adamez, J. Bussman, A. M. van der Sar, G. W. Otto, R. Geisler, and H. P. Spaink. 2005. Transcriptome profiling of adult zebrafish at the late stage of chronic tuberculosis due to *Mycobacterium marinum* infection. *Mol. Immunol.* 42: 1185–1203.
66. Zhu, Z., T. Zheng, R. J. Homer, Y. K. Kim, N. Y. Chen, L. Cohn, Q. Hamid, and J. A. Elias. 2004. Acidic mammalian chitinase in asthmatic Th2 inflammation and IL-13 pathway activation. *Science* 304: 1678–1682.
67. Elias, J. A., R. J. Homer, Q. Hamid, and C. G. Lee. 2005. Chitinases and chitinase-like proteins in T_H2 inflammation and asthma. *J. Allergy Clin. Immunol.* 116: 497–500.